Med Chem Res (2013) 22:1147–1162
DOI 10.1007/s00044-012-0116-9

MEDICINAL CHEMISTRY RESEARCH

ORIGINAL RESEARCH

Synthesis and biological evaluation of new curcumin derivatives as antioxidant and antitumor agents

Said M. Bayomi · Hassan A. El-Kashef · Mahmoud B. El-Ashmawy · Magda N. A. Nasr · Magda A. El-Sherbeny · Farid A. Badria · Laila A. Abou-zeid · Mariam A. Ghaly · Naglaa I. Abdel-Aziz

Received: 4 January 2012 / Accepted: 22 May 2012 / Published online: 7 June 2012

Abstract Twenty-four new compounds were prepared, taking curcumin as a lead, in order to explore their antioxidant and antitumor properties. The capacities of these derivatives to scavenge the 2,2′-azinobis(3-ethylbenzothiazoline-6-sulfonic acid) radical cation ($ABTS^{\cdot+}$), and to protect human red blood cells (RBCs) from oxidative haemolysis were investigated. In addition, the percentage viability of different cell lines (Hep G2, WI38, VERO and MCF-7) was tested. The result of the antitumor testing was generally in accordance with those of the antioxidant assays. Compounds which bear *o*-methoxy substitution to the 4-hydroxy function in the phenyl ring (**7g**, **5g** and **3g**) exhibited significantly higher $ABTS^{\cdot+}$-scavenging, antihaemolysis, and antitumor activities than other derivatives. In addition, molecular modelling studies were carried out for biologically active and inactive compounds, to study the structure–activity relationship, with the aim to elucidate which portions of the molecules are critical for the antioxidant and antitumor activity.

S. M. Bayomi · M. B. El-Ashmawy · M. A. El-Sherbeny · M. A. Ghaly · N. I. Abdel-Aziz (✉)
Department of Medicinal Chemistry, Faculty of Pharmacy, Mansoura University, Mansoura 35516, Egypt
e-mail: naglaabdalaziz2005@yahoo.com

H. A. El-Kashef
Department of Pharmacology, Faculty of Pharmacy, Mansoura University, Mansoura 35516, Egypt

M. N. A. Nasr · L. A. Abou-zeid
Department of Pharmaceutical Organic Chemistry, Faculty of Pharmacy, Mansoura University, Mansoura 35516, Egypt

F. A. Badria
Department of Pharmacognosy, Faculty of Pharmacy, Mansoura University, Mansoura 35516, Egypt

Keywords Curcumin · Synthesis · Free radical scavenging · Antihaemolytic effect · Antitumor effect · Molecular modelling studies

Introduction

The area of free radical biology and medicine is developing fast, since the discovery of the involvement of free radicals in oxidative tissue injury and diseases. Free radicals and other reactive oxygen species such as superoxide radical anion, hydroxyl radical and hydrogen peroxide, are constantly generated through many biological processes and may be considered as a measure of biological inefficiency. The human body uses an antioxidant system to neutralize the excessive levels of reactive oxygen species that consists of enzymes such as superoxide dismutases, catalases and glutathione peroxidases, in addition to numerous non-enzymatic small molecules that are widely distributed in the biological system such as glutathione, α-tocopherol, ascorbic acid, β-carotene and selenium (Memon and Sudheer, 2007). In general, the cell is able to maintain an appropriate balance between oxidants and antioxidants under normal conditions. The imbalance between reactive oxygen species production and the available antioxidant defence leads to a widely accepted phenomenon called oxidative stress (Djordjevic, 2004).

Curcumin (1,7-bis(4-hydroxy-3-methoxyphenyl)-1,6-heptadiene-3,5-dione) is a naturally occurring phenolic compound isolated as a yellow pigment from turmeric (dry rhizomes of *Curcuma longa*, Zingiberaceae) which is commonly used as a food colorant, spice and traditional medicine in India and China (Geol *et al*., 2008; Sharma *et al*., 2005). This compound has been the focus of many recent biochemical investigations due to its various biological and pharmacological properties, including antioxidant

(Lee *et al*., 2009; Venkatesan and Rao, 2000) and anticancer activities (Aggarwal *et al*., 2003). The cancer preventive capability of curcumin is linked to its direct antioxidant ability to eliminate free radicals and to reduce oxidative stress (Dinkova-Kostova and Talalay, 2008). Consequently, the past few years have witnessed tremendous interest in the antioxidant activity of curcumin. The structural simplicity and nontoxicity of curcumin, along with its defects such as poor bioavailability (Anand *et al*., 2007), made this molecule a promising lead compound for development of potential antioxidant and cancer chemopreventive agents (Fadda *et al*., 2010; Liang *et al*., 2009).

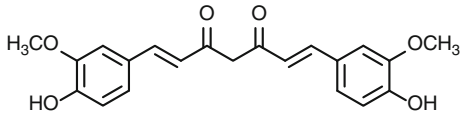

Curcumin

In this study, different series of curcumin derivatives were synthesized (Schemes 1, 2) and their antioxidant activity were assessed by $ABTS^{\cdot+}$-scavenging and antihaemolysis experiments. To explore the substituent effect, type and distribution pattern, and the role of central active methylene hydrogens, compounds **3a**–**g** and **4** were synthesized, where the seven carbon spacer was retained. Compounds **5a**–**g** and **5h**–**j** were prepared to test the effect of decreasing length and flexibility of the seven carbon spacer. Fused pyrano ring systems were built in compounds **6a**–**g** to simulate coumarin and flavonoid ring systems, which are well known for their antioxidant and anticarcinogenic activities (Guthrie and Carroll, 1998). Finally, certain fused pyrazoles **7e**–**g**, **8a**–**e** and **8h**–**j**, were included to formulate a more comprehensive structure–activity relationship, if any.

Results and discussion

Chemistry

The synthetic routes of the designed compounds are illustrated in Schemes 1 and 2. Dimethylation of pentane-2,4-dione using dimethyl sulphate in dimethylsulfoxide (DMSO) and tetrahydrofuran (THF) as solvent, in the presence of potassium carbonate, afforded 3,3-dimethylpentane-2,4-dione **1**, which was used directly in an aldol condensation with various aromatic aldehydes **2a**–**g** in ethanolic sodium hydroxide solution to yield the corresponding 4,4-dimethyl-1,7-bis((substituted)phenyl)hepta-1,6-diene-3,5-diones **3a**–**g** (Scheme 1). Refluxing curcumin with diethyl sulphate in acetone, in the presence of anhydrous potassium carbonate, afforded 1,7-bis(4-ethoxy-3-methoxyphenyl)-4,4-diethylhepta-1,6-diene-3,5-dione **4** (Scheme 1).

On the other hand, aldol condensation of cyclohexanone or cycloheptanone with different aromatic aldehydes

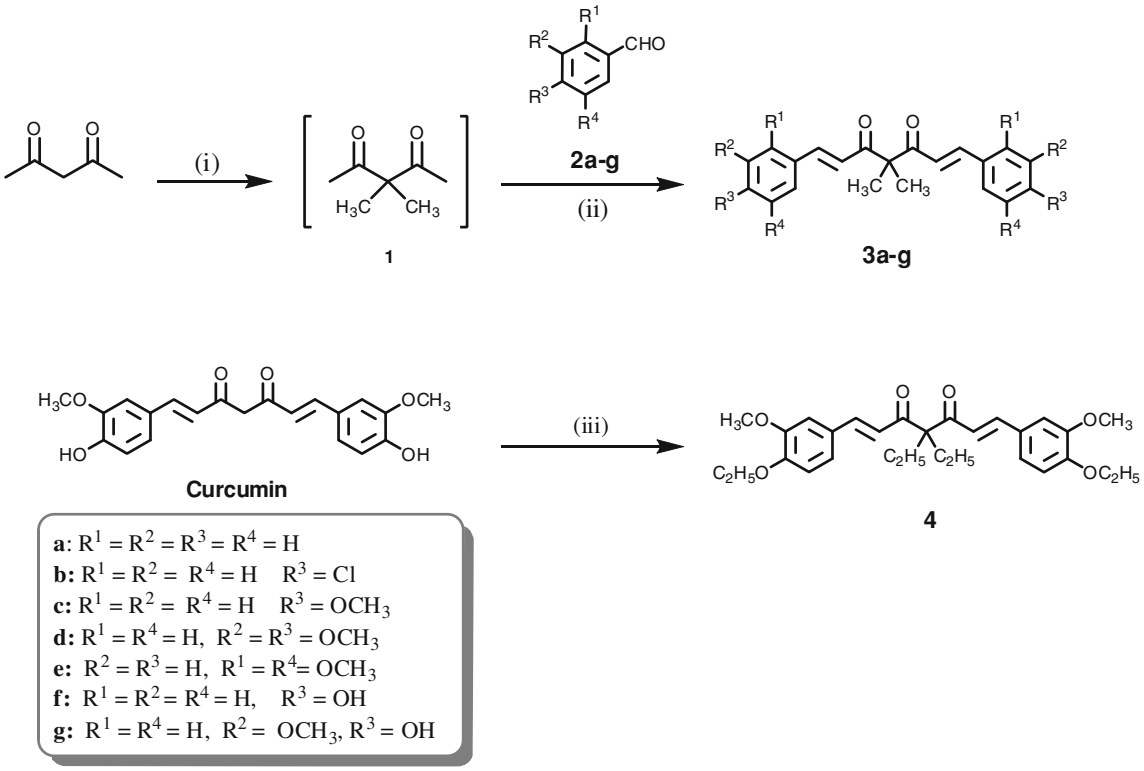

Scheme 1 Reaction protocol for the synthesis of **3a**–**g** and **4**: (*i*) $(CH_3)_2SO_4$, K_2CO_3, DMSO/THF; (*ii*) NaOH, EtOH; (*iii*) $(C_2H_5)_2SO_4$, acetone, K_2CO_3

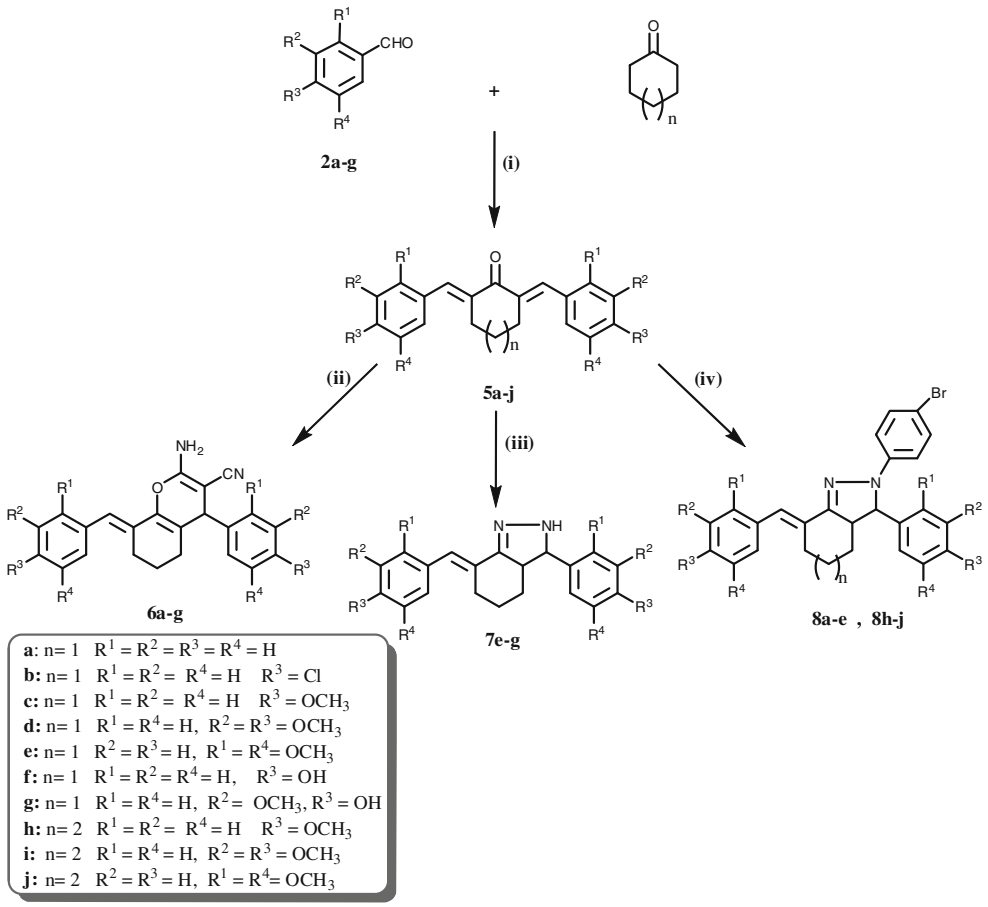

Scheme 2 Reaction protocol for the synthesis of **5a–j**, **6a–g**, **7e–g**, **8a–e** and **8h–j**: (*i*) NaOH, EtOH; (*ii*) malononitril, butanol or malononitril, DMF, piperidine; (*iii*) hydrazine hydrate, EtOH; (*iv*) 4-bromo phenylhydrazine hydrochloride, Na ethoxide, EtOH

(**2a–e**) in an ethanolic sodium hydroxide solution afforded 2,6-bis((substituted) benzylidene)cyclohexanone **5a–e** and 2,7-bis(substituted benzylidene)cycloheptanones **5h–j**, respectively. The previously reported compounds **5f** and **5g** were obtained via the interaction of cyclohexanone with the hydroxybenzaldehydes **2f** and **2g**, respectively, in glacial acetic acid and concentrated hydrochloric acid.

Condensation of 2,6-bis(4-methoxybenzylidene)cyclohexanone **5c** with malononitrile in *n*-butanol afforded 2-amino-8-(4-methoxybenzylidene)-4-(4-methoxyphenyl)-5,6,7,8-tetrahydro-4*H*-chromene-3-carbonitrile **6c**. On the other hand, the interaction of other 2,6-bis((substituted) benzylidene)cyclohexanones **5a**, **b**, **d–g** with malononitrile was done in dimethylformamide (DMF) in the presence of piperidine at room temperature, to get the corresponding 5,6,7,8-tetrahydro-4*H*-chromene-3-carbonitriles, **6a**, **b**, **d–g**.

Finally, cyclocondensation of **5e–g** using hydrazine hydrate in refluxing ethanol afforded 7-(substituted benzylidene)-3-(substituted phenyl)-3,3a,4,5,6,7-hexahydro-2*H*-indazoles **7e–g**. Cyclocondensation of 2,6-bis((substituted) benzylidene)cyclohexanones **5a–e** and 2,7-bis(substituted benzylidene)cycloheptanones **5h–j** with 4-bromophenylhydrazine hydrochloride in absolute ethanol in the presence of sodium ethoxide yielded 2-(4-bromophenyl)-7-((substituted)benzylidene)-3-((substituted)phenyl)-3,3a,4,5,6,7-hexahydro-2*H*-indazoles **8a–e** and (*E*)-2-(4-bromophenyl)-8-(substituted benzylidene)-3-(substituted phenyl)-2,3,3a,4,5,6,7,8-cyclohepta[c]pyrazoles **8h–j**, respectively (Scheme 2).

Biological evaluation

Assay for 2,2′-azinobis(3-ethylbenzothiazoline-6-sulfonic acid) radical ($ABTS^{\cdot+}$) scavenging activity

The antioxidant activity assay employed here is one of the several assays that depend on measuring the consumption of stable free radicals, to evaluate the free radical scavenging activity of the investigated compound. The methodology assumes that consumption of the stable free radical ($X^{\cdot}$) by hydrogen-donating antioxidants (YH) will be determined by reaction as follows:

$$X^{\cdot} + YH \rightarrow XH + Y^{\cdot}.$$

The rate and/or the extent of the process measured in terms of the decrease in $X^{\cdot}$ concentration, would be related to the ability of the added compounds (YH) to trap free radicals. The decrease in colour intensity of the free radical solution

due to scavenging of the free radical by the antioxidant material is measured colourimetrically at a specific wavelength. The assay employs the radical cation derived from 2,2′-azinobis(3-ethylbenzothiazoline-6-sulfonic acid) (ABTS) as stable free radical. The advantage of ABTS-derived free radical method over other methods is that the produced colour remains stable for more than 1 h and the reaction is stoichiometric (Chyong *et al*., 2011; Lissi *et al*., 1999). In this study, all the synthesized compounds were subjected to ABTS test (Table 1).

Table 1 The percentage inhibition of the ABTS radical cation by the tested compounds

Compound Nos.	% inhibition
Control of ABTS	0
Ascorbic acid	80.81
Curcumin	87.64
3a	4.84
3b	2.32
3c	7.75
3d	12.59
3e	3.68
3f	28.68
3g	52.9
4	26.35
5a	1.93
5b	0.58
5c	1.35
5d	0
5e	1.16
5f	9.49
5g	74.22
5h	1.74
5i	0.77
5j	5.03
6a	0.19
6b	1.55
6c	0.38
6d	16.86
6e	0.38
6f	16.66
6g	57.75
7e	25.6
7f	54.45
7g	76.74
8a	1.74
8b	2.9
8c	5.03
8d	0.19
8e	0.77
8h	3.1
8i	0.96
8j	3.1

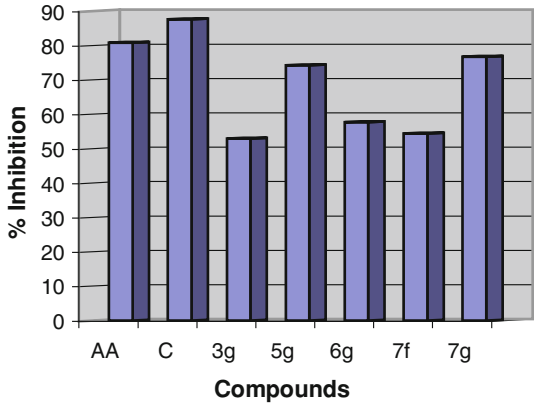

AA ascorbic acid, *C* curcumin

From these results, it is concluded that compounds **7g**, **5g**, **6g**, **7f** and **3g** exhibited more than 50 % inhibition of the ABTS radical cation. The latter compounds, except compound **7f**, share an *o*-methoxy substituent to the 4-hydroxy function on the two aryl rings, though the core of the molecules is completely different. Thus, the length and the shape of the spacer between the two aryl rings could be varied without affecting the scavenging activity. However, compound **7f**, characterized by having a pyrazole ring, appears amongst the most active compounds indicating that the pyrazole NH might have a role in trapping the ABTS free radical. The antioxidant activity of the previously prepared compound **5g** was also determined and proved to be effective (Lee *et al*., 2009; Shang *et al*., 2010; Ligeret *et al*., 2004; Weber *et al*., 2006).

Antihaemolysis assay

Human red blood cells (RBCs) are heterogeneous media, and are particularly exposed to endogenous oxidative damage because of their specific role as oxygen carriers. RBC membrane is rich in polyunsaturated fatty acids which are very susceptible to free radical-mediated peroxidation. AAPH (2,2′-azobis(2-amidinopropane) dihydrochloride) has been extensively used as a free radical initiator for biological studies because it is water-soluble and the rate of free radical generation from AAPH can be easily controlled and measured. Thermal decomposition of AAPH in the aqueous dispersion of RBCs produces an initiating radical

Table 2 The percentage reduction of RBCs haemolysis after preincubation with these nine tested compounds at 2 μg/ml

Compound Nos.	% Reduction of RBCs haemolysis
Ascorbic acid	17.6
Curcumin	50.4
3g	98.0
5a	42.2
5g	66.8
6a	63.2
6b	60.2
6c	80.2
6e	70.4
7f	81.0
7g	94.8

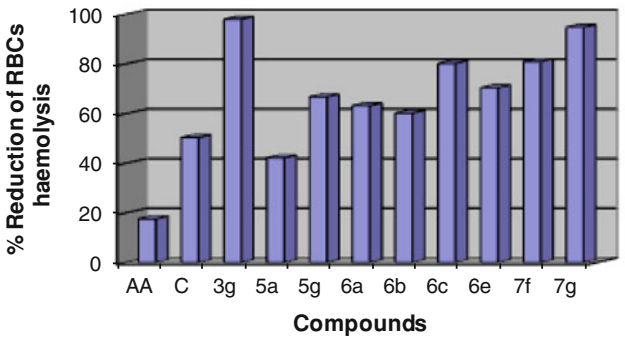

AA ascorbic acid, *C* curcumin

($R^{\cdot}$) which can attack the polyunsaturated lipids (LH) in RBC membranes to induce lipid peroxidation. Since the lipid peroxidation is a free radical chain reaction, the RBC membrane is quickly damaged, leading to haemolysis. On the other hand, whether antioxidants (YH) are present or added to RBCs, they would react with the chain propagating peroxyl radicals ($LOO^{\cdot}$) to stop the peroxidation, hence inhibit haemolysis (Shang *et al*., 2010). Data obtained from haemolysis assay indicated that the most of the tested compounds produced 100 % haemolysis and hence excluded from the antihaemolysis assay. Hence, only nine compounds, that did not induce haemolysis, were subjected to the antihaemolysis assay (Table 2).

From these results, it is concluded that compounds showing the highest protective activity towards AAPH-induced oxidative RBCs haemolysis could be arranged as follows: **3g** > **7g** > **7f** > **6c** > **6e** > **5g** > **6a** > **6b** > curcumin. Compounds **3g** and **7g** are nearly equipotent. They share the *o*-methoxy substituent to the 4-hydroxy function, while the core of the two molecules is completely different. Thus, the length and the shape of the spacer between the two aryl rings could be varied without affecting activity. Compounds **7**, bearing resemblance to coumarin and flavonoid ring systems, comprise four active members in the antihaemolysis assay. This may focus on the importance of the pyrano-fused system in the in vitro assay. While curcumin was the most active compound in the ABTS assay, many compounds preceeded it in the antihaemolysis assay. These compounds vary in their structures from compounds retaining the seven carbon spacer between the two aryl rings, to compounds having a 2*H*-indazole or chromene ring embedded, to compounds having a saturated cyclohexane ring core. This may reflect the versatility of the active structures in the antihaemolysis assay.

Antitumor testing

The synthesized curcumin analogues were subjected to antitumor testing by measuring their effect on the percentage viability of four different cell lines; human hepatocellular liver carcinoma cell line (hep G2), human lung fibroblast cell line (WI38), kidney epithelial cells of the African green monkey (VERO), and human breast adenocarcinoma cell line (MCF-7) (Kálai *et al*., 2011). All the synthesized compounds were subjected to antitumor testing. Among the tested compounds, only compounds **3d**, **3e**, **3f**, **3g**, **4**, **5f**, **5g**, **6d**, **6f**, **6g**, **7e**, **7f** and **7g** exhibited promising activity against the different cell lines used, while the rest of compounds showed no activity (Table 3).

In this study, the obtained data indicated that the most active compounds against hep G2 cell line were in the following order: curcumin ≈ **6d** > **7g** > **5g** > **3g** > **3f**. On the other hand, compounds **6d**, curcumin, **5g**, **7g**, **3d** and **5f** proved to be effective against WI38 cell line. Moreover, VERO cell line was found to be sensitive toward compounds **7g**, curcumin, **6d**, **5g**, **3e** and **7f**, while compounds **7g**, **6d**, **5g**, **3g**, and **3f** are particularly effective against MCF-7 cell line. In all types of cell lines, antitumor activity seems to be inherent to compounds **7g**, **6d** and **5g**, the first two exceeded curcumin in some cell lines. The cyclic curcumin analogues **7g** and **5g** retain the *o*-methoxyphenoxy moiety as a common structure. This may reflect the importance of such moiety in antitumor activity. However, the spacer between the two aryl rings differs from that of curcumin. It is noteworthy that compound **5g** was previously tested for its cytotoxic activity (Liang *et al*., 2009), and also proved effective. The notable feature being the superiority of the chromene structure **6d**, even over curcumin, though it lacks the hydroxyl functions. In conclusion, the results of the antitumor testing were generally in accordance with those of the antioxidant assays. Compounds which bear *o*-methoxy substitution to the 4-hydroxy function (**7g**, **5g** and **3g**) exhibited significantly higher $ABTS^{\cdot+}$-scavenging, antihaemolysis and antitumor activities than other derivatives.

Table 3 The results of the antitumor assay of curcumin and its tested analogues, together with 5-fluorouracil (5FU) as positive control, at 20 μg/ml, on the percentage viability of the different cell lines

Compound Nos.	Hep G2	WI38	VERO	MCF-7
5FU	0	0	0	0
Curcumin	18	51	24	19
3d	78	75	89	87
3e	84	80	74	79
3f	57	88	82	64
3g	47	78	82	55
4	78	82	88	94
5f	88	77	84	74
5g	28	58	69	32
6d	19	12	65	21
6f	78	79	83	82
6g	81	84	82	79
7e	78	100	67	82
7f	89	88	76	75
7g	21	65	12	19

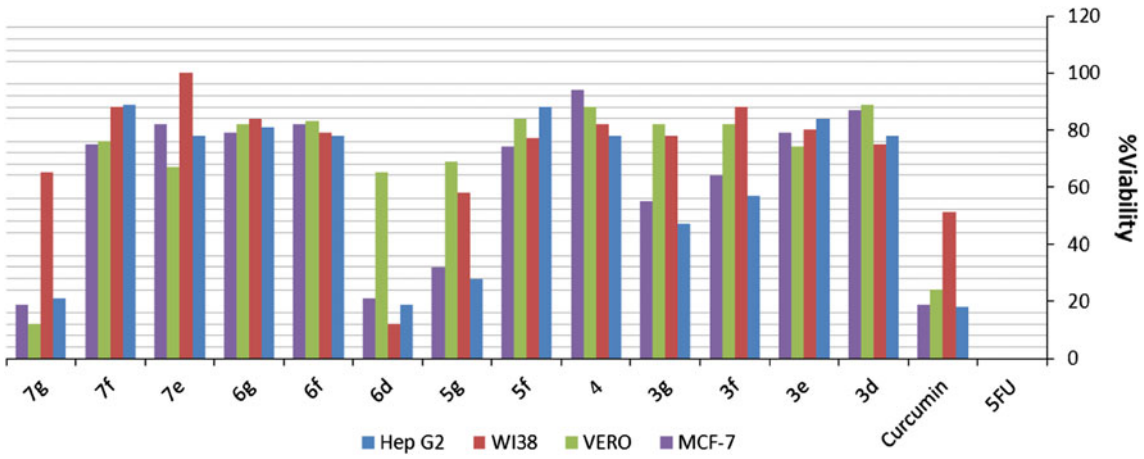

5FU 5-fluorouracil, *C* curcumin

Molecular modelling discussion

Conformational analyses of most of the prepared compounds were performed, then flexible alignment, and electrostatic and hydrophobic mappings were applied for certain selected compounds, based on the biological results.

Stochastic conformational analysis

Stochastic conformational search was performed using the global minima conformers of the most active analogues, the moderately active analogues, and the inactive analogue of each series to confirm the proper conformational features responsible for the corresponding biological activities.

*Compounds **3a–g***

Compounds **3a–g** with the seven carbon spacer bridge between the two (substituted)phenyl terminal groups showed that **3g**, the most active analogue in this series, exhibited a common alignment similar to the lead ligand 'curcumin'. The 4,4-dimethyl substitution showed negligible interference with the degree of flexibility of the carbon bridge spacer. The three middle carbons of the carbon bridge spacer got in narrow zigzag angle keeping the *trans* configuration and the proper distance between the two benzylidene rings.

3g

Compound ***4***

Compound **4**, with the seven carbon spacer bridge between the two substituted phenyl terminal groups, exhibited a common alignment similar to the lead ligand 'curcumin'. The flexibility of the carbon spacer bridge with the conjugated double bonds and the diketones represented the important structural characteristic. However, the 4,4-diethyl substitution played steric features with the degree of flexibility of carbon bridge spacer where the angular configuration of the carbon spacer got smaller, with certain extent, keeping the two benzylidene rings in zigzag orientation keeping the *trans* configuration around each double bond.

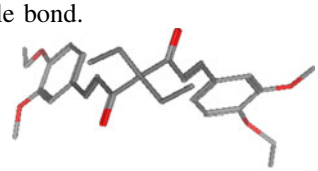

4

Compounds ***5a–g*** *and* ***5h–j***

Compound **5g**, with the bis(benzylidene)cyclohexanone, showed the geometry of the lowest energy conformer 'global minima' with the *trans* configuration arranged in a comparable manner to that of the lead ligand keeping the proper distance between the two terminal benzylidene rings.

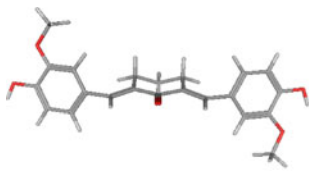

5g

Compounds ***6a–g***

Compounds **6a–g**, with the five carbon spacer bridge between the two (substituted)phenyl terminal groups, showed that **6g**, the most active analogue in this series, exhibited limited flexibility due to the steric feature of tetrahydro-4*H*-chromene ring keeping the chance of conformational change restricted to the angular position to the terminal (4-hydroxy-3-methoxy)benzylidene ring and this may explain the slightly impaired biological efficacy of the members of this series.

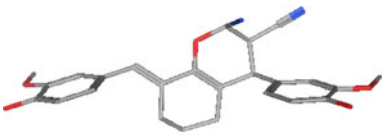

6g

Compounds ***7f*** *and* ***7g***

Both members of this series represent the most biologically active analogues of the entire tested compounds. The hexahydro-2*H*-indazole ring performed certain degree of flexibility besides the angular conformational freedom of the terminal benzylidene ring. The global minima conformer kept the common structural features with the same distance between the two terminal disubstituted phenyl groups similar to the corresponding rings of the lowest energy conformer of the lead analogue 'curcumin'.

7g

Compounds ***8a–e*** *and* ***8h–j***

All the compounds, **8a–e** and **8h–j**, showed limited conformational changes due to occupying the five carbon spacer bridge with the hexahydro-2*H*-indazole ring keeping the chance of free conformational change restricted to the angular position to the terminal benzylidene ring; however, the hexahydro-2*H*-indazole ring still reserves certain elasticity degree. *N*2 substitution with 4-bromophenyl ring prompted high field of steric energy supporting the clarification of the abolishing reactivity of these group analogues.

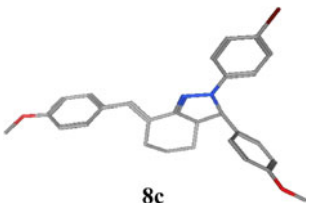

8c

Flexible alignment

Flexible alignment was performed to gain an insight into the fingerprint features responsible for the different

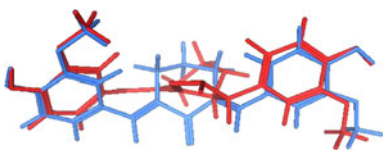

Fig. 1 Flexible alignment of the most active compounds: **7g** (in *red*) and **5g** (in *blue*) (Color figure online)

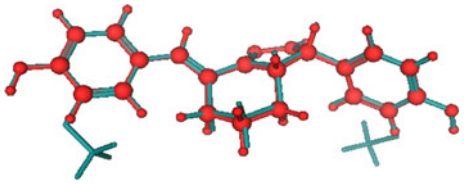

Fig. 2 Flexible alignment of the moderately active compound **7f** (in *red*) and the most active compound **7g** (in *blue*) (Color figure online)

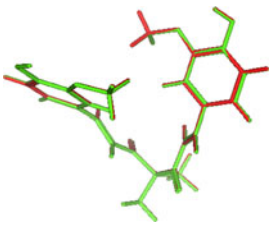

Fig. 3 Flexible alignment of the moderately active compound **3g** (in *green*) and curcumin (in *red*) (Color figure online)

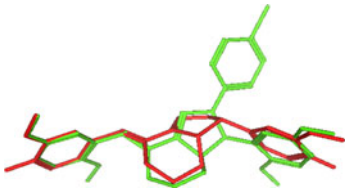

Fig. 4 Flexible alignment of the least active compound **8e** (in *green*) and the most active compound **7g** (in *red*) (Color figure online)

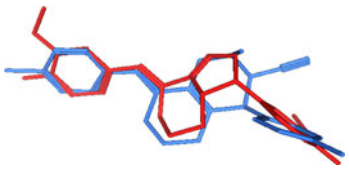

Fig. 5 Flexible alignment of the least active compound **6b** (in *blue*) and the most active compound **7g** (in *red*) (Color figure online)

biological activities. The structures of the most active compounds **7g** and **5g**, with different structural cores, were subjected to the flexible alignment techniques.

Flexible alignment of the most active compounds; ***7g*** *and* ***5g***

Mapping the MOE-generated alignment conformer (MOE, 2007.9 of Chemical Computing Group. Inc.,) indicated the proper superposition of the two phenyl rings. The disubstituted functional groups; 4-hydroxy and 3-methoxy were aligned with high scoring. Another fingerprint factor of proper alignment is the five carbon spacer length present in both the compounds. Moreover, the 2*H*-indazole of compound **7g** and the corresponding cyclohexyl ring of compound **5g** were deviated to certain extent showing the restricted flexibility of the indazole ring in comparison with the cyclohexyl moiety referring to the free rotation around single double bond that are missing in compound **7g**. Compound **7g** showed high electrostatic field due to the N-atom rich indazole ring. Both **7g** and **5g** possessed better free radical scavenging, antihaemolytic and antitumor activities and that may be expressed as a comparative relationship between the activity and the better alignment represented by the lower score value of the configuration (Fig. 1).

Flexible alignment of the moderately active compounds; ***7f*** *and* ***3g***

Analysis of the moderately active analogues highlights the common fingerprint features that are essential for elucidation of the relative changing of the obtained activity. Compound **7f** showed identical alignment with the most active analogue **7g** except the absence of 3-methoxy group that seemed to be essential functional feature for proper biological activity. The other features are totally accommodating the two structures with proper alignment score, including the 4-phenoxy group with the spacer distance of five carbons (Fig. 2).

Compound **3g** is curcumin analogue with the dimethyl substitution at C4 of the seven carbon spacer bridge. The introducing of 4,4-dimethyl groups caused moderate activity as antitumor and antioxidant agent. On the other hand, the presence of donating 4,4-dimethyl groups improved the antihaemolysis activity to the maximal extent. The alignment of **3g** with its putative ligand was highly scored (Fig. 3).

Flexible alignment of the inactive compounds; ***8e*** *and* ***6b***

Examining the degree of similarity between the most active analogue **7g** and the least active compound **8e** indicated that the common features of alignment were the indazole core; a flexible hydrophilic area, in addition to the benzylidene fragment and the terminal phenyl group; the hydrophobic area that performed proper alignment in all the active analogues. The least active **8e** has *N*2 of pyrazole attached to *p*-bromophenyl moiety that introduced bulkiness to the total surface area and led to increment of the steric energy. Moreover, changing the position on two terminal phenyl groups with 2,5-dimethoxy substitution instead of 3,4-disubstitution impaired all the given biological activities (Fig. 4).

Configurational analysis of the alignment data base regarding the structural feature behind the abolishing of the antioxidant, antitumor activities of compound **6b** indicated that the presence of 5,6,7,8-tetrahydro-4*H*-chromene ring instead of the indazole ring played restrained effect to the biological activity, in addition to the introduction of 4-chloro substitution instead of 4-hydroxy and 3-methoxy disubstitution groups. Even the cyano and amino substitutions at the 4*H*-chromene ring improved the hydrophilic

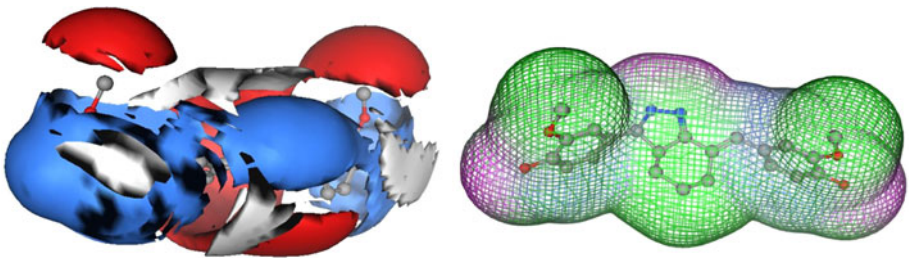

Fig. 6 Electrostatic map (*left*) and hydrophobic map (*right*) for the most active compound **7g**

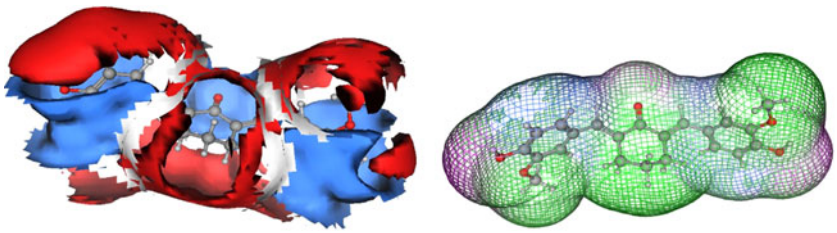

Fig. 7 Electrostatic map (*left*) and hydrophobic map (*right*) for the most active compound **5g**

effect but the overall structural changes did not fulfil the required alignment features (Fig. 5).

Electrostatic and hydrophobic mappings

Mapping the electrostatic, hydrophobic and the donor/acceptor hydrogen bond characteristics were performed using the lowest energy conformer obtained from the geometrically constrained conformational search, in an attempt to understand the variant degree of biological reactivity of the tested compounds according to the electrostatic feature mappings. The electrostatic feature map is an application of the Poisson–Boltzmann equation (PBE) to the prediction of electrostatically preferred locations of hydrophobic, H-bond acceptor, and H-bond donor locations. Electrostatically positive regions (donor) are coloured blue, negative regions (acceptor) are coloured red, and neutral regions are coloured white.

*Predicting electrostatically favourable regions and hydrophobic regions of the most active analogues **7g** and **5g***

Electrostatic mapping of **7g** showed that the disubstituted 3-methoxy groups capped the functional groups representing the acceptor regions and coloured red. The presence of *N*1 and *N*2 of the indazole ring represented donor regions (in blue). Hydrophilic predictions are coloured purple and hydrophobic predictions are coloured green. The hydrophobic distributions of the most active compound **7g** had two phenyl fragments and appeared green, while the presence of the hydroxyl, methoxy and the nitrogen indazole groups represented the hydrophilic distributions and appeared purple (Fig. 6).

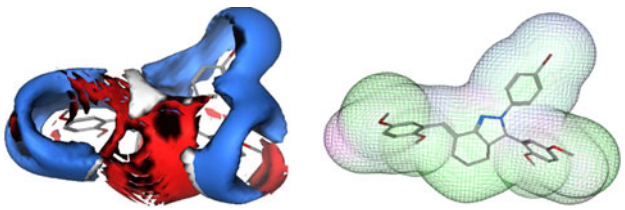

Fig. 8 Electrostatic map (*left*) and hydrophobic map (*right*) for the least active compound **8e**

Electrostatic mapping of compound **5g** showed the presence of 3-methoxy and the carbonyl oxygen groups representing the acceptor regions that were coloured red. Phenyl and cyclohexyl fragments were represented as white neutral region. 4-Hydroxy groups showed donor profile and were coloured blue. The hydrophobic distributions of the most active compound **5g** had two phenyl and cyclohexyl fragments that appeared green. On the other hand, the hydroxyl and methoxy groups represented the hydrophilic distributions and appeared purple (Fig. 7).

As a result, the most active compounds **7g** and **5g** can adopt conformations with identical orientations and sufficient agreement of the electrostatic and the hydrophobic potential patterns.

*Predicting electrostatically favourable regions and hydrophobic regions of the least active analogues **8e** and **6b***

Electrostatic mapping of **8e** showed that the disubstituted 2,5-dimethoxy groups distributed the electrostatic features turning the ortho, meta positions into an acceptor region (red). The presence of the 4-bromophenyl ring performed electrostatic donating behaviour turning the protruded area into donor regions (blue). Varying the electrostatic

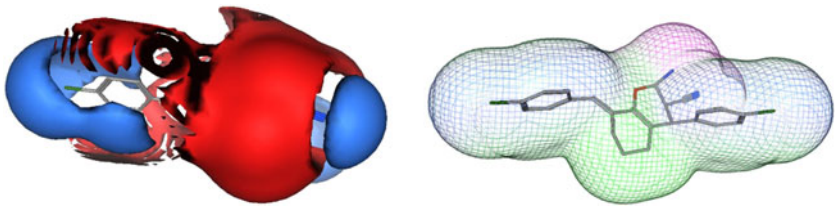

Fig. 9 Electrostatic map (left) and hydrophobic map (right) for the least active compound **6b**

Table 4 Calculated Lipinski's rule of five for the most active compounds

Compound Nos.	ABTS assay	Antihaemolysis	Antitumor	Parameter			
				a-don	a-acc	M. Wt.	Log *P*
3g	6	1	4	2.0000	6.0000	396.439	5.094
5g	3	6	3	2.0000	5.0000	366.413	4.177
7f	5	3	Moderate	3.0000	3.0000	319.384	3.349
7g	2	2	1	3.0000	5.0000	379.436	3.331
Curcumin	1	9	1	2.0000	6.0000	368.385	3.718

a-acc number of H-bond acceptor, *a-don* number of H-bond donor, *Log P* calculated lipophilicity, *M. Wt.* molecular weight

distribution differently in comparison with the electrostatic performance of the most active analogue **7g**, designate the significant elucidation concerning the abolishing of the biological activity of compound **8e.** The hydrophobic distributions (coloured green) of the least active compound **8e** are due to the presence of three phenyl fragments, while the methoxy and the nitrogen indazole groups represent the hydrophilic distributions (coloured purple), but located and distributed differently in comparison with the most active analogue **7g** (Fig. 8).

Electrostatic mapping of **6b** showed that the di-*para*-chloro substituted groups distributed the electrostatic features turning the *para* positions into a donor region (blue). Presence of the rigid fused tetrahydro-4*H*-chromene ring sited Van der Waal's force that located heavily in a different manner in comparison with the most active analogue **7g**. The cyano and amino groups assumingly enrich the electrostatic interaction but located away from the favourable considered area revealing to some extent the reason of abolishing of the biological activity of compound **6b**. The hydrophobic distributions (coloured green) of the least active compound **6b** are highly expressed due to the presence of firm tetrahydro-4*H*-chromene ring and two phenyl fragments, while the cyano and the amino groups represent the hydrophilic distributions (coloured purple), but located and distributed differently in comparison with the most active analogue **7g** (Fig. 9).

Lipinski's rule of five

The introduction of Lipinski's 'rule of five' has initiated a profound shift in the thinking paradigm of medicinal chemists. Lipinski's rule of five is a rule of thumb to evaluate drug likeness, or determine if a chemical compound with a certain pharmacological or biological activity has properties that would make it a likely orally active drug in humans. The rule was formulated by Lipinski et al. in (1997), based on the observation that the most medication drugs are relatively small and lipophilic molecules. The rule is important for drug development where a pharmacologically active lead structure is optimized step-wise for increased activity and selectivity, as well as drug-like properties as described by Lipinski's rule. The modification of the molecular structure often leads to drugs with higher molecular weight, more rings, more rotatable bonds, and a higher lipophilicity (Oprea *et al.*, 2001). Lipinski's rule says that, in general, an orally active drug has no more than one violation of the following criteria:

- Not more than 5 hydrogen bond donors (nitrogen or oxygen atoms with one or more hydrogen atoms)
- Not more than 10 hydrogen bond acceptors (nitrogen or oxygen atoms)
- A molecular weight under 500 Da
- An octanol–water partition coefficient log *P* of less than 5.

It is noteworthy that all numbers are multiples of five, which is the origin of the rule's name. Computational studies were completed to evaluate the obedience of the most active compounds to the Lipinski's rule of five and the results showed that all investigated compounds obey these rules (Table 4) and these compounds should present good passive oral absorption. The lipophilic characters of the investigated compounds are in agreement with their biological activities.

Conclusion

Twenty-four new compounds have been synthesized and subjected to antioxidant and antitumor screening. The obtained data revealed that compounds which bear *o*-methoxy substitution to the 4-hydroxy function (**7g**, **5g** and **3g**) exhibited significantly higher $ABTS^{\cdot+}$-scavenging, antihaemolysis, and antitumor activities than other derivatives. Conformational analyses, flexible alignment, and electrostatic and hydrophobic mappings were applied and were in agreement with the experimental results.

Experimental protocols

Synthetic procedures

Melting points (°C) were recorded using a *Fisher–Johns* melting point apparatus and are uncorrected. Microanalyses were performed in the Microanalytical unit, Cairo University. IR spectra (KBr) were recorded on Mattson 5000 FT-IR spectrometer (ν in cm^{-1}). ^1H NMR spectra were obtained on FT-NMR spectrometer (200 MHz) Gemini Varian using TMS as internal standard (chemical shifts in ppm, δ units). MS analyses were performed on JEOL JMS-600H spectrometer. Thin layer chromatography (TLC) was performed on silica gel G for TLC (Merck) and spots were visualized by irradiation with ultraviolet light (UV; 254 nm). Curcumin was purchased from Fluka. The syntheses of compounds **3a** (Weber *et al*., 2005), **3d** (Roughley and Whiting, 1973), **5a** (Singh *et al*., 2009), **5b** (Singh *et al*., 2009), **5c** (Wang *et al*., 2004), **5d** (Singh *et al*., 2009), **5f** (Du *et al*., 2006), **5g** (Du *et al*., 2006), **5h** (Singh *et al*., 2009), **5i** (Singh *et al*., 2009), **6a** (Zhou, 2003), and **6b** (Zhou, 2003), have been previously reported.

*General method for synthesis of 4,4-dimethyl-1,7-bis ((substituted)phenyl)-hepta-1,6-diene-3,5-diones (**3b**, **c**, **e–g**)* To a cooled solution (10 °C) of 2,4-pentanedione (1.33 g, 13.3 mmol) in DMSO (7 ml) and THF (4 ml), potassium carbonate (4.60 g, 33.4 mmol) was added. Dimethyl sulphate (2.12 g, 16.8 mmol) was added dropwise while stirring and the mixture was stirred at room temperature for 3 days. The expected 3,3-dimethylpentane-2,4-dione **1**, was used in the next step without isolation. To the stirred reaction mixture, a solution of the appropriate aromatic aldehyde **2b**, **c**, **e–g** (26.6 mmol) in ethanol (20 ml) was added. Ethanolic sodium hydroxide (50 ml, 10 %) was added dropwise, and stirred overnight at room temperature. After completion of the reaction (TLC), the mixture was poured onto ice–water, then conc. HCl was added dropwise until effervescence and precipitation ceased. The precipitated solid was collected by filtration, air dried, and recrystallized from ethyl acetate. For compounds **3f**, **g**, the residue obtained was purified on silica gel preparative TLC plates using chloroform/methanol (9:1) as an eluent.

*4,4-Dimethyl-1,7-bis(4-chlorophenyl)-hepta-1,6-diene-3, 5-diones (**3b**)*. Yield, 40 %; mp 155–157 °C; IR (KBr) ν_{max}/cm^{-1} 1682 (C=O), 1599 (C=C). ^1H NMR ($CDCl_3$); δ: 1.26 (s, 6H, $2CH_3$), 7.26–8.07 (m, 12H, 8Ar-H and 4 alkenyl CH). MS *m/z* (%); 374, $[M + H]^+$ (9.14), 44 (100.00). Anal. Calcd for $C_{21}H_{18}Cl_2O_2$ (%):C, 67.57; H, 4.86. Found: C, 67.90; H, 4.56.

*4,4-Dimethyl-1,7-bis(4-methoxyphenyl)-hepta-1,6-diene-3,5-diones (**3c**)*. Yield, 52 %; mp 126–128 °C; IR (KBr) ν_{max}/cm^{-1} 1677 (C=O), 1598 (C=C).^1H NMR ($CDCl_3$); δ: 1.25 (s, 6H, $2CH_3$), 3.87 (s, 6H, $2OCH_3$), 6.95 (d, 2H, 2 alkenyl CH), 7.25–7.86 (m, 8H, 8ArH), 8.06 (d, 2H, 2 alkenyl CH). MS *m/z* (%); 364, M^+ (6.09), 121 (100.00). Anal. Calcd for $C_{23}H_{24}O_4$ (%):C, 75.80; H, 6.64. Found: C, 76.23; H, 6.87.

*4,4-Dimethyl-1,7-bis(2,5-dimethoxyphenyl)-hepta-1,6-diene-3,5-diones (**3e**)*. Yield, 45 %; mp 67–69 °C; IR (KBr) ν_{max}/cm^{-1} 1685 (C=O), 1602 (C=C). ^1H NMR ($CDCl_3$); δ: 1.26 (s, 6H, $2CH_3$), 3.93 (s, 12H, $4OCH_3$), 6.89 (d, 2H, 2 alkenyl CH), 7.06–7.59 (m, 6H, 6Ar-H), 7.76 (d, 2H, 2 alkenyl CH). MS *m/z* (%); 425, M^+ (1.25), 55 (100.00). Anal. Calcd for $C_{25}H_{28}O_6$ (%):C, 70.74; H, 6.65. Found: C, 70.59; H, 6.34.

*4,4-Dimethyl-1,7-bis(4-hydroxyphenyl)-hepta-1,6-diene-3,5-diones (**3f**)*. Yield, 40 %; mp 80–82 °C; ^1H NMR ($CDCl_3$); δ: 1.22 (s, 6H, $2CH_3$), 6.83–7.74 (m, 12H, 8Ar-H and 4 alkenyl CH), 9.76 (s, 2H, 2OH). MS *m/z* (%); 337, $[M + H]^+$ (0.86), 63 (100.00). Anal. Calcd for $C_{21}H_{20}O_4$ (%):C, 74.98; H, 5.99. Found: C, 75.43; H, 5.57.

*4,4-Dimethyl-1,7-bis(4-hydroxy-3-methoxyphenyl)-hepta-1,6-diene-3,5-diones (**3g**)*. Yield, 45 %; mp 56–58 °C; IR (KBr) ν_{max}/cm^{-1} 1683 (C=O), 1600 (C=C). ^1H NMR ($CDCl_3$); δ: 1.30 (s, 6H, $2CH_3$), 3.82 (s, 6H, $2OCH_3$), 6.80 (d, 2H, 2 alkenyl CH), 7.10–7.79 (m, 8H, 6Ar-H and 2 alkenyl CH), 10.00 (s, 2H, 2OH). MS *m/z* (%); 396, M^+(13.96), 55 (100.00). Anal. Calcd for $C_{23}H_{24}O_6$ (%): C, 69.68; H, 6.10. Found: C, 70.00; H, 6.41.

*General method for the synthesis of 1,7-bis(4-ethoxy-3-methoxyphenyl)-4,4-diethylhepta-1,6-diene-3,5-dione (**4**)* Anhydrous potassium carbonate (2 g) was added to a stirred solution of curcumin (1.72 g, 5 mmol) in acetone (100 ml), followed by diethyl sulphate (1.43 g, 9 mmol). The mixture was heated at reflux temperature while stirring for 22 h. Potassium carbonate was then filtered off, and the solvent was evaporated. The residue was washed with diethyl ether, and crystallized from ethanol to give compound **4.** Yield, 42 %; mp 125–127 °C. IR (KBr) ν_{max}/cm^{-1} 1625 (C=O). ^1H NMR ($CDCl_3$); δ: 1.42 (t, 6H, $2CH_2CH_3$), 1.66 (t, 6H, $2OCH_2CH_3$), 2.35 (q, 4H, $2CH_2CH_3$), 4.10 (s, 6H, $2OCH_3$), 4.31 (q, 4H, $2OCH_2CH_3$),

6.67 (d, 2H, 2 alkenyl CH), 6.96–7.49 (m, 6H, 6Ar-H), 7.78 (d, 2H, 2 alkenyl CH). MS *m/z* (%); 481, M^+ (3.65), 69 (100.00). Anal. Calcd for $C_{29}H_{36}O_6$ (%): C, 72.48; H, 7.55. Found: C, 72.90; H, 8.02.

*General method for the synthesis of (2E, 6E)-bis(2,5-dimethoxybenzylidene)cyclohexanone (**5e**)* To a mixture of cyclohexanone (0.98 g, 10 mmol) and 2,5-dimethoxybenzaldehyde **2e** (3.32 g, 20 mmol), ethanolic sodium hydroxide solution (50 ml, 10 %) was added dropwise. The mixture was stirred at room temperature for 2 h, then refrigerated overnight. The separated solid was collected by filtration, washed with water, dried and recrystallized from ethanol to give the title compound **5e**. Yield, 91 %; mp 130–131 °C. IR (KBr) ν_{max}/cm^{-1} 1601 (C=O). ^1H NMR ($CDCl_3$); δ: 1.22 (m, 2H, CH_2), 2.60 (t, 4H, $2CH_2$), 3.80 (s, 12H, $4OCH_3$), 6.80–7.59 (m, 8H, 6ArH and 2 ylidene CH). Anal. Calcd for $C_{24}H_{26}O_5$ (%): C, 73.08; H, 6.64. Found: C, 73.07; H, 6.76.

*General method for the synthesis of (2E, 7E)-bis(2,5-dimethoxybenzylidene)cycloheptanone (**5j**)* To a mixture of cycloheptanone (1.12 g, 10 mmol) and 2,5-dimethoxybenzaldehyde **2e** (3.32 g, 20 mmol), ethanolic sodium hydroxide solution (50 ml, 10 %) was added dropwise. The mixture was stirred at room temperature for 2 h, then refrigerated overnight. The separated solid was collected by filtration, washed with water, dried and recrystallized from ethanol to give the title compound **5j**. Yield, 53 %; mp 122–124 °C. IR (KBr) ν_{max}/cm^{-1} 1604 (C=O). ^1H NMR ($CDCl_3$); δ: 1.77 (m, 4H, $2CH_2$), 2.85 (t, 4H, $2CH_2$), 3.80 (s, 12H, $4OCH_3$), 6.86–6.89 (m, 4H, 4ArH), 7.27 (s, 2H, 2ArH), 7.94 (s, 2H, 2 ylidene CH). MS *m/z* (%); 408, M^+ (17.90), 229 (100.00). Anal. Calcd for $C_{25}H_{28}O_5$ (%): C, 73.51; H, 6.91. Found: C, 73.72; H, 6.04.

*General method for the synthesis of (E)-2-amino-8-((substituted)benzylidene)-4-((substituted)phenyl)-5,6,7,8-tetrahydro-4H-chromene-3-carbonitriles (**6c–g**)* A mixture of the appropriate 2,6-bis(substituted benzylidene) cyclohexanone **5d–g** (1 mmol) and malononitrile (0.28 g, 4 mmol) in DMF (7 ml) and piperidine (4 drops) was stirred at room temperature for 24 h. The reaction mixture was then concentrated. The precipitated solid was collected by filtration and recrystallized from methanol (**6e** and **g**). For compounds **6d** and **6f**, purification on silica gel preparative thin layer chromatographic plates was done using *n*-hexane/ethyl acetate 1:1 as an eluent, and recrystallization was done from ethanol.

*For compound **6c*** A mixture of 2,6-bis(4-methoxybenzylidene)cyclohexanone **5c** (0.334 g, 1 mmol) and malononitrile (0.07 g, 1 mmol) in *n*-butanol (10 ml) was heated under reflux for 26 h. The precipitated product was filtered and recrystallized from ethanol to yield compound **6c**.

*(E)-2-amino-8-(4-methoxybenzylidene)-4-(4-methoxyphenyl)-5,6,7,8-tetrahydro-4H-chromene-3-carbonitriles (**6c**)*. Yield, 40 %; mp 211–213 °C. IR (KBr) ν_{max}/cm^{-1} 3465 and 3367 (NH_2), 2187 (C≡N), 1670, 1631, 1600 (C=C), 1249 (C–N). ^1H NMR ($CDCl_3$); δ: 1.11 (m, 2H, CH_2), 2.72 (m, 4H, $2CH_2$), 3.78,3.81 (s, 6H, $2OCH_3$), 4.00 (s, 1H, pyran H), 6.11 (br s, 2H, NH_2, D_2O exchangeable), 6.45–7.10 (m, 9H, 8Ar-H and ylidene CH). MS *m/z* (%); 399, M^+-1 (29.4), 147 (100.00). Anal. Calcd for $C_{25}H_{24}N_2O_3$ (%): C, 74.98; H, 6.04; N, 7.00. Found: C, 75.00; H, 6.32; N, 6.74.

*(E)-2-amino-8-(3,4-dimethoxybenzylidene)-4-(3,4-dimethoxyphenyl)-5,6,7,8-tetrahydro-4H-chromene-3-carbonitriles (**6d**)*. Yield, 55 %; mp 145–147 °C. IR (KBr) ν_{max}/cm^{-1} 3389 and 3324 (NH_2), 2185 (C≡N), 1668, 1638, 1603 (C=C), 1249 (C–N).^1H NMR ($CDCl_3$); δ: 1.20 (m, 2H, CH_2), 2.72 (t, 4H, $2CH_2$), 3.75, 3.81 (s, 12H, $4OCH_3$), 3.91 (s, 1H, pyran H), 5.81 (br s, 2H, NH_2, D_2O exchangeable), 6.58–7.20 (m, 7H, 6Ar-H and ylidene CH). Anal. Calcd for $C_{27}H_{28}N_2O_5$ (%): C, 70.42; H, 6.13; N, 6.08. Found: C, 70.75; H, 6.35; N, 6.25.

*(E)-2-amino-8-(2,5-dimethoxybenzylidene)-4-(2,5-dimethoxyphenyl)-5,6,7,8-tetrahydro-4H-chromene-3-carbonitriles (**6e**)*. Yield, 64 %; mp 218–219 °C. IR (KBr) ν_{max}/cm^{-1} 3408 and 3331 (NH_2), 2191 (C≡N), 1676, 1645, 1608 (C=C), and 1224 (C–N).^1H NMR ($CDCl_3$); δ: 1.32 (m, 2H, CH_2), 2.89 (t, 4H, $2CH_2$), 3.70; 3.75 (s, 12H, $4OCH_3$), 4.40 (s, 1H, pyran H), 6.56–7.02 (m, 7H, 6ArH and ylidene CH), 8.32 (br s, 2H, NH_2, D_2O exchangeable). Anal. Calcd for $C_{27}H_{28}N_2O_5$ (%): C, 70; H, 6.13; N, 6.08. Found: C, 69.71; H, 6.35; N, 6.18.

*(E)-2-amino-8-(4-hydroxybenzylidene)-4-(4-hydroxyphenyl)-5,6,7,8-tetrahydro-4H-chromene-3-carbonitriles (**6f**)*. Yield, 40 %; mp 128–130 °C. IR (KBr) ν_{max}/cm^{-1} 3616 (OH), 3433 and 3342 (NH_2), 2192 (C≡N), 1670, 1635, 1595 (C=C), and 1263 (C–N).^1H NMR ($CDCl_3$); δ: 1.20 (m, 2H, CH_2), 3.19 (t, 4H, $2CH_2$), 3.52 (s, 2H, NH_2, exchangeable), 4.17 (s, 1H, pyran H), 6.66–7.84 (m, 9H, 8Ar-H and ylidene CH), 8.56 (s, 2H, 2OH, D_2O exchangeable). Anal. Calcd for $C_{23}H_{20}N_2O_3$ (%): C, 74.18; H, 5.41; N, 7.52. Found: C, 74.29; H, 5.39; N, 7.89.

*(E)-2-amino-8-(4-hydroxy-3-methoxybenzylidene)-4-(4-hydroxy-3-methoxyphenyl)-5,6,7,8-tetrahydro-4H-chromene-3-carbonitriles (**6g**)*. Yield, 40 %; mp 178–179 °C. ^1H NMR ($CDCl_3$); δ: 1.42 (m, 2H, CH_2), 2.89 (t, 4H, $2CH_2$), 3.74; 3.77 (s, 6H, $2OCH_3$), 3.84 (s, 1H, pyran H), 6.54–6.88 (m, 7H, 6ArH and ylidene H), 8.89 (s, 2H, NH_2, D_2O exchangeable), 9.12 (s, 2H, 2OH, D_2O exchangeable). MS *m/z* (%); 432, M^+ (17.63), 55 (100.00). Anal. Calcd for

$C_{25}H_{24}N_2O_5$ (%): C, 69.43; H, 5.59; N, 6.48. Found: C, 69.16; H, 5.72; N, 6.33.

*General method for the synthesis of (E)-7-(substituted benzylidene)-3-(substituted phenyl)-3,3a,4,5,6,7-hexahydro-2H-indazoles (**7e–g**)* A mixture of the 2,6-diarylidenecyclohexanones **5e–g** (1 mmol), and hydrazine hydrate (1 ml, 20 mmol) in absolute ethanol (15 ml) was heated at reflux while stirring for 21 h. The reaction mixture was then evaporated, and the residue obtained was washed with water, collected by filtration, dried, and recrystallized from ethanol to yield the title compounds.

*(E)-7-(2,5-dimethoxybenzylidene)-3-(2,5-dimethoxyphenyl)-3,3a,4,5,6,7-hexahydro-2H-indazoles (**7e**)*. Yield, 78 %; mp 70–71 °C. IR (KBr) ν_{max}/cm^{-1} 3338 (N–H), 1593 (C=N), 1497 (C=C), 1221(C–N). ^1H NMR ($CDCl_3$); δ: 1.55–3.42 (m, 7H, aliphatic), 4.25 (s, 12H, $4OCH_3$), 5.00 (br s, 1H, NH, D_2O exchangeable), 5.32 (dd, 1H, NCH), 7.26–7.72 (m, 7H, 6Ar-H and ylidene CH). Anal. Calcd for $C_{24}H_{28}N_2O_4$ (%): C, 70.57; H, 6.91; N, 6.86. Found: C, 70.32; H, 6.85; N, 7.02.

*(E)-7-(4-hydroxybenzylidene)-3-(4-hydroxyphenyl)-3,3a,4,5,6,7-hexahydro-2H-indazoles (**7f**)*. Yield, 90 %; mp 166–168 °C. IR (KBr) ν_{max}/cm^{-1} 3272 (N–H), 1606 (C=N), 1510 (C=C), 1237 (C–N). ^1H NMR ($CDCl_3$); δ: 1.41–3.41 (m, 7H, aliphatic), 5.32 (br s, 1H, NH, D_2O exchangeable), 5.52 (dd, 1H, NCH), 7.23–7.85 (m, 9H, 8Ar-H and ylidene CH), 9.8 (s, 2H, 2OH). MS *m/z* (%); 320, M^+ (3.67), 215 (100.00). Anal. Calcd for $C_{20}H_{20}N_2O_2$ (%): C, 74.98; H, 6.29; N, 8.74. Found: C, 74.65; H, 6.60; N, 8.47.

*(E)-7-(4-hydroxy-3-methoxybenzylidene)-3-(4-hydroxy-3-methoxyphenyl)-3,3a,4,5,6,7-hexahydro-2H-indazoles (**7g**)*. Yield, 53 %; mp 179–180 °C. IR (KBr) ν_{max}/cm^{-1} 3342 (N–H), 1604 (C=N), 1514 (C=C), 1270 (C–N). ^1H NMR ($CDCl_3$); δ: 1.50–3.31 (m, 7H, aliphatic), 3.90 (s, 6H, $2OCH_3$), 5.10 (br s, 1H, NH, D_2O exchangeable), 5.40 (dd, 1H, NCH), 7.22–7.82 (m, 7H, 6Ar-H and ylidene CH), 10.00 (s, 2H, 2OH). MS *m/z* (%); 380, M^+ (26.37), 378, M^+-2 (100.00). Anal. Calcd for $C_{22}H_{24}N_2O_4$ (%): C, 69.46; H, 6.36; N, 7.36. Found: C, 69.21; H, 6.53; N, 7.71.

*General method for the synthesis of (E)-2-(4-bromophenyl)-7-((substituted)benzylidene)-3-((substituted)phenyl)-3,3a,4,5,6,7-hexahydro-2H-indazoles (**8a–e**)* A mixture of the appropriate 2,6-bis((substituted)benzylidene)cyclohexanones **5a–e** (1 mmol), 4-bromophenylhydrazine hydrochloride (0.671 g, 3 mmol), and sodium ethoxide (0.408 g, 6 mmol) in absolute ethanol (20 ml) was heated under reflux for 20 h. The reaction mixture was then filtered and the filtrate was concentrated. The separated solid was collected by filtration, washed with water, and recrystallized from ethanol.

*(E)-2-(4-bromophenyl)-7-(benzylidene)-3-(phenyl)-3,3a,4,5,6,7-hexahydro-2H-indazoles (**8a**)*. Yield, 50 %; mp 168–169 °C. ^1H NMR ($CDCl_3$); δ: 1.32–3.15 (m, 7H, aliphatic), 4.55 (d, 1H, NCH), 6.86–7.46 (m, 15H, 14Ar-H and ylidene CH). Anal. Calcd for $C_{26}H_{23}BrN_2$ (%): C, 70.43; H, 5.23; N, 6.32. Found: C, 69.92; H, 5.28; N, 6.25.

*(E)-2-(4-bromophenyl)-7-(4-chlorobenzylidene)-3-(4-chlorophenyl)-3,3a,4,5,6,7-hexahydro-2H-indazoles (**8b**)*. Yield, 55 %; mp 98–100 °C. ^1H NMR ($CDCl_3$); δ: 1.08–3.08 (m, 7H, aliphatic), 4.51 (d, 1H, NCH), 6.64–7.58 (m, 13H, 12Ar-H and ylidene CH). Anal. Calcd for $C_{26}H_{21}BrCl_2N_2$ (%): C, 60.96; H, 4.13; N, 5.47. Found: C, 59.41; H, 4.38; N, 5.80.

*(E)-2-(4-bromophenyl)-7-(4-methoxybenzylidene)-3-(4-methoxyphenyl)-3,3a,4,5,6,7-hexahydro-2H-indazoles (**8c**)*. Yield, 45 %; mp 70–72 °C. IR (KBr) ν_{max}/cm^{-1} 1589 (C=N), 1499 (C=C), 1221 (C–N). ^1H NMR ($CDCl_3$); δ: 1.12–3.13 (m, 7H, aliphatic), 3.73 (s, 3H, OCH_3); 3.78 (s, 3 H, OCH_3), 4.71 (d, 1H, NCH), 6.55–7.80 (m, 13H, 12Ar-H and ylidene CH). MS *m/z* (%);503, M^+ (3.54), 135 (100.00). Anal. Calcd for $C_{28}H_{27}BrN_2O_2$ (%): C, 66.80; H, 5.41; N, 5.56. Found: C, 67.02; H, 5.33; N, 5.14.

*(E)-2-(4-bromophenyl)-7-(3,4-dimethoxybenzylidene)-3-(3,4-dimethoxyphenyl)-3,3a,4,5,6,7-hexahydro-2H-indazoles (**8d**)*. Yield, 45 %; mp 178–179 °C. IR (KBr) ν_{max}/cm^{-1} 1595 (C=N), 1499 (C=C), 1227 (C–N).). ^1H NMR ($CDCl_3$); δ: 1.11–3.45 (m, 7H, aliphatic), 3.72; 3.77; 4.72 (s, 12 H, $4OCH_3$), 5.17 (d, 1H, NCH), 6.52–7.85 (m, 11H, 10Ar-H and ylidene CH). Anal. Calcd for $C_{30}H_{31}BrN_2O_4$ (%): C, 63.95; H, 5.55; N, 4.97. Found: C, 63.70; H, 5.27; N, 4.40.

*(E)-2-(4-bromophenyl)-7-(2,5-dimethoxybenzylidene)-3-(2,5-dimethoxyphenyl)-3,3a,4,5,6,7-hexahydro-2H-indazoles (**8e**)*. Yield, 60 %; mp 87–89 °C. IR (KBr) ν_{max}/cm^{-1} 1588 (C=N), 1494 (C=C), 1219 (C–N).^1H NMR ($CDCl_3$); δ: 1.12–3.46 (m, 7H, aliphatic), 3.73; 3.78; 4.82 (s, 12H, $4OCH_3$), 5.07 (d, 1H, NCH), 6.42–7.80 (m, 11H, 10Ar-H and ylidene CH). MS *m/z* (%); 563, M^+ (9.13), 212 (100.00). Anal. Calcd for $C_{30}H_{31}BrN_2O_4$ (%): C, 63.95; H, 5.55; N, 4.97. Found: C, 63.67; H, 5.46; N, 4.87.

*General method for the synthesis of (E)-2-(4-bromophenyl)-8-((substituted) benzylidene)-3-((substituted) phenyl)-2,3,3a,4,5,6,7,8-cyclohepta[c]pyrazoles (**8h–j**)* A mixture of the appropriate 2,7-bis(substituted benzylidene)cycloheptanones **5h–j** (1 mmol), 4-bromophenylhydrazine hydrochloride (0.671 g, 3 mmol), and sodium ethoxide (0.408 g, 6 mmol) in absolute ethanol (20 ml) was heated under reflux for 20 h. The reaction mixture was then filtered and the filtrate was concentrated. For compounds **8h** and **8i**, purification on silica gel preparative TLC plates, using *n*-hexane/ethyl acetate 1:1 as an eluent was done, followed by crystallization from ethanol. For compound **8j**,

the ethanolic filtrate was diluted with water, then extracted with chloroform (3 × 10 ml). The residue after evaporation was recrystallized from methanol.

*(E)-2-(4-bromophenyl)-8-(4-methoxybenzylidene)-3-(4-methoxyphenyl)-2,3,3a,4,5,6,7,8-cyclohepta[c] pyrazoles (**8h**)*. Yield, 50 %; mp 53–55 °C. IR (KBr) ν_{max}/cm^{-1} 1600 (C=N), 1500 (C=C), 1247 (C–N). ^1H NMR ($CDCl_3$); δ: 1.21–3.16 (m, 9H, aliphatic), 3.84 (s, 6 H, $2OCH_3$), 4.19 (d, 1H, NCH), 6.48–7.76 (m, 13H, 12Ar-H and ylidene CH). MS *m/z* (%); 517, M^+ (2.61), 398 (100.00). Anal. Calcd for $C_{29}H_{29}BrN_2O_2$ (%): C, 67.31; H, 5.65; N, 5.41. Found: C, 67.52; H, 5.34; N, 5.15.

*(E)-2-(4-bromophenyl)-8-(3,4-dimethoxybenzylidene)-3-(3,4-dimethoxyphenyl)-2,3,3a,4,5,6,7,8-cyclohepta [c]pyrazoles (**8i**)*. Yield, 50 %; mp 58–60 °C. ^1H NMR ($CDCl_3$); δ: 1.20–3.18 (m, 9H, aliphatic), 3.71; 3.84; 3.87; 3.90 (s, 12 H, $4OCH_3$), 4.29 (d, 1H, NCH), 6.58–7.66 (m, 11H, 10Ar-H and ylidene CH). MS *m/z* (%); 577, M^+ (9.45), 426 (100.00). Anal. Calcd for $C_{31}H_{33}BrN_2O_4$ (%): C, 64.47; H, 5.76; N, 4.85. Found: C, 64.23; H, 5.42; N, 5.00.

*(E)-2-(4-bromophenyl)-8-(2,5-dimethoxybenzylidene)-3-(2,5-dimethoxyphenyl)-2,3,3a,4,5,6,7,8-cyclohepta [c]pyrazoles (**8j**)*. Yield, 50 %; mp 77–79 °C. IR (KBr) ν_{max}/cm^{-1} 1592 (C=N), 1497 (C=C), 1228 (C–N). ^1H NMR ($CDCl_3$); δ: 1.21–3.19 (m, 9H, aliphatic), 3.70; 3.84; 3.89; 3.91 (s, 12 H, $4OCH_3$), 4.30 (d, 1H, NCH), 6.62–7.86 (m, 11H, 10Ar-H and ylidene CH). MS *m/z* (%); 577, M^+ (2.00), 377 (100.00). Anal. Calcd for $C_{31}H_{33}BrN_2O_4$ (%):C, 64.47; H, 5.76; N, 4.85. Found: C, 64.05; H, 5.80; N, 4.61.

Biological testing

ABTS test

A mixture of solution of ABTS (2 ml, 0.1 g/100 ml, Sigma-Aldrich, St. Louis, MO, USA) and solution of MnO_2 (3 ml, 25 mg/ml), prepared in phosphate buffer (pH 7, 0.1 M, BP 1998) was shaken, centrifuged, and decanted. The absorbance ($A_{control}$) of the resulting green-blue solution ($ABTS^{\cdot+}$ radical solution) was recorded at λ_{max} 734 nm. The absorbance (A_{test}) was measured upon the addition of 20 µl of 1 mg/ml solution of the test sample in spectroscopic grade MeOH/buffer (1:1 v/v) to the ABTS solution. The decrease in absorbance is expressed as % inhibition which is calculated from the equation:

$$\%\ \text{inhibition} = \frac{A_{control} - A_{test}}{A_{control}} \times 100.$$

Ascorbic acid 20 µl (2 mM) solution was used as standard antioxidant (positive control). Blank sample was run using solvent without ABTS.

Antihaemolysis assay

Human RBCs were separated from heparinised blood that was drawn from a healthy volunteer. The blood was centrifuged at 2,000 rpm for 10 min to separate the RBCs from plasma, then the RBCs were washed three times with phosphate-buffered saline (PBS) at pH 7.4. During the last washing, the cells were centrifuged at 2,000 rpm for 10 min to obtain a constantly packed cell volume. The 5 % suspension of RBCs in PBS (pH 7.4) was incubated under air atmosphere at 37 °C for 5 min, into which the tested compounds dissolved in DMSO were added to be examined for their direct haemolytic effect. The reaction mixture was shaken gently while being incubated at 37 °C. The extent of haemolysis was determined spectrophotometrically (Kuang *et al*., 1994); where aliquots of the reaction mixture were taken out at appropriate time intervals, diluted with 0.15 M NaCl, and centrifuged at 2,000 rpm for 10 min to separate the RBCs. The percentage haemolysis was determined by measuring the absorbance of haemoglobin in the supernatant at 540 nm and compared with that of complete haemolysis by treating the same RBC suspension with distilled water. The final concentration of DMSO was 0.1 % (v/v) that did not interfere with the determination. Every experiment was repeated five times. Compounds which caused haemolysis were excluded from the next step of the experiment. Other compounds were evaluated for their ability to protect RBCs from AAPH-induced oxidative damage (antihaemolysis assay). The procedure was repeated, where the test compounds, dissolved in DMSO, were added and incubated for 30 min before addition of a PBS solution of AAPH (50 mM) (Sigma-Aldrich, St. Louis, MO, USA).

Antitumor testing

The cells were grown in suspension culture, partly floating and partly attached, in Roswell Park Memorial Institute (RPMI) 1640 medium (Sigma chemical Co., St. Louis, USA), supplemented with 10 % foetal bovine serum (GIBCO, UK). They were maintained at 37 °C in a humidified atmosphere with 5 % CO_2. The viability of the cells used in control experiments (DMSO only without drug) exceeded 95 % as determined with trypan blue. Test compounds were prepared initially at concentration of 1 mg/ml DMSO.

Molecular modelling methodology

Construction of the molecular structure of the lead ligand and the synthesized analogues

Putative lead ligand ‘curcumin’ and the synthesized compounds were constructed from fragment libraries using the

builder module of MOE. The partial atomic charges for each analogue were assigned with the semiempirical mechanical calculation method 'AM1' implemented in MOE. Each structure was energy minimised and geometrically optimized by using the MMFF94 force field with gradient 0.05.

Conformational search and the derived structural global minima

The partially charged and energy minimised structures of the tested compounds were subjected to conformational search using the stochastic conformational search module implemented in MOE (El-Sherbeny *et al*., 2010, Al-Omary *et al*., 2010). Such search was performed without chiral conversion and with using chiral constraints around the double bonds using the energy cutoff 10 Å, the dihedral minimization RMS gradient 100 kcal/mol Å and the Cartesian minimization RMS gradient 0.001 kcal/mol Å. The iteration limit was allowed to 1000 iterations where the root mean square (RMS) tolerance fixed to 0.1 kcal/mol Å. The conformers with the lowest energy were selected as the global minima for further modelling studies.

Flexible alignment search

The fingerprint key structural features of the global minima conformers of the selected analogues were determined using the implemented flexible alignment search module (Labute *et al*., 2001, Halgren, 1996). The iteration limit was set to 200 iterations for each compound, turning on the option of preserving the geometrical configuration of the double bond centers using the MMFF94 force field optimization energy to get proper alignment feature analysis.

Acknowledgments The authors extend their appreciation to Mansoura University research center for funding this study.

References

Aggarwal BB, Kumar A, Bharti AC (2003) Anticancer potential of curcumin: preclinical and clinical studies. Anticancer Res 23:363–398

Al-Omary FAM, Abou-zeid LA, Nagi MN, Habib EE, Abdel-Aziz AA-M, El-Azab AS, Abdel-Hamide SG, Al-Omar MA, Al-Obaid AM, El-Subbagh HI (2010) Non-classical antifolates. Part 2. Synthesis, biological evaluation, and molecular modeling study of some new 2,6-substituted quinazolin-4-ones. Bioorg Med Chem 18:2849–2863

Anand P, Kunnumakkara AB, Newman RB, Aggarwal BB (2007) Bioavailability of curcumin: problems and promises. Mol Pharm 4:807–818

Chyong FH, Hui P, Cédric B, Jadranka T-S, Paul A (2011) $ABTS^{\cdot+}$ scavenging activity of polypyrrole, polyaniline and poly(3,4-ethylenedioxythiophene). Polym Int 60:69–77

Dinkova-Kostova AT, Talalay P (2008) Direct and indirect antioxidant properties of inducers of cytoprotective proteins. Mol Nutr Food Res 52:5128–5138

Djordjevic VB (2004) Free radical in cell biology. Int Rev Cytol 237:57–89

Du Z, Liu R, Shao W, Mao X, Ma L, Gu L, Huang Z, Cham ASC (2006) α-Glucosidase inhibition of natural curcuminoids and curcumin analogs. Eur J Med Chem 41:213–218

El-Sherbeny MA, Abdel-Aziz AA-M, Ahmed MA (2010) Synthesis and antitumor evaluation of novel diarylsulfonylurea derivatives: molecular modeling applications. Eur J Med Chem 45:689–697

Fadda AA, Badria FA, El-Attar KM (2010) Synthesis and evaluation of curcumin analogues as cytotoxic agents. Med Chem Res 19:413–430

Geol A, Kunnumakkara AB, Aggarwal BB (2008) Curcumin as "curecumin": from kitchen to clinic. Biochem Pharm 75: 787–809

Guthrie N, Carroll KK (1998) Inhibition of mammary cancer by citrus flavonoids. In: Manthey JA, Buslig BS (eds) Flavonoids in the living system. Plenum, New York, p 227

Halgren TAJ (1996) Merck molecular force field. I. Basis, form, scope, parameterization, and performance of MMFF94. J Comput Chem 17:490–519

Kálai T, Kuppusamy ML, Balog M, Selvendiran K, Rivera BK, Kuppusamy P, Hideg K (2011) Synthesis of *N*-substituted 3,5-bis(arylidene)-4-piperidones with high antitumor and antioxidant activity. J Med Chem 54:5414–5421

Kuang ZH, Wang PF, Zheng RL, Liu Z, Liu Y (1994) Making vitamin C liposoluble enhances its protective effect against radical induced hemolysis of erythrocytes. Chem Phys Lipids 91:95–97

Labute P, Williams C, Feher M, Sourial E, Schmidt JM (2001) Flexible alignment of small molecules. J Med Chem 44:1483–1490

Lee K, Ab Aziz FH, Syahida A, Abas F, Shaari K, Israf DA, Lajis NH (2009) Synthesis and biological evaluation of curcumin-like diarylpentanoid analogues for anti-inflammatory, antioxidant and antityrosinase activities. Eur J Med Chem 44:3195–3200

Liang G, Shao L, Wang Y, Zhao C, Chu Y, Xiao J, Zhao Y, Li X, Yang S (2009) Exploration and synthesis of curcumin analogues with improved structural stability both in vitro and in vivo as cytotoxic agents. Bioorg Med Chem 17:2623–2631

Ligeret H, Barthelemy S, Zini R, Tillement J, Labidalle S, Morin D (2004) Effects of curcumin and curcumin derivatives on mitochondrial permeability transition pore. Free Radic Biol Med 36:919–929

Lipinski CA, Lombardo F, Dominy BW, Feeney PJ (1997) Experimental and computational approaches to estimate solubility and permeability in drug discovery and development settings. Adv Drug Del Rev 23:3–25

Lissi E, Modak B, Torres R, Escobar J, Urzua A (1999) Total antioxidant potential of resinous exudates from *Heliotropium* species, and a comparison of ABTS and DPPH methods. Free Radic Res 30:471–477

Memon VP, Sudheer AR (2007) Antioxidant and anti-inflammatory properties of curcumin. In: Aggarwal BB, Surh Y, Shishodia S (eds) The molecular targets and therapeutic uses of curcumin in health and disease. Springer, New York, pp 106–107

MOE 2007.9 of Chemical Computing Group. Inc.

Oprea TI, Davis AM, Teague SJ, Leeson PD (2001) Is there a difference between leads and drugs? A historical perspective. J Chem Inf Comput Sci 41:1308–1315

Roughley PJ, Whiting DA (1973) Experiments in the biosynthesis of curcumin. J Chem Soc Perkin Trans 1(20):2379–2388

Shang Y, Jin X, Shang X, Tang J, Liu G, Dai F, Qian Y, Fan G, Liu Q, Zhou B (2010) Antioxidant capacity of curcumin-directed

analogues: structure–activity relationship and influence of microenvironment. Food Chem 119:1435–1442

Sharma RA, Gescher AJ, Verma WP (2005) Curcumin: the story so far. Eur J Cancer 41:1958–1968

Singh N, Pandey J, Yadav A, Chaturvedi V, Bhatnagar S, Gaikwad AN, Sinha SK, Kumar A, Shukla PK, Tripathi RT (2009) A facile synthesis of α,α'-(EE)-bis(benzylidene)-cycloalkanones and their antitubercular evaluations. Eur J Med Chem 44: 1705–1709

Venkatesan P, Rao MN (2000) Structure–activity relationships for the inhibition of lipid peroxidation and the scavenging of free radicals by synthetic symmetrical curcumin analogues. J Pharm Pharmacol 52:1123–1128

Wang L, Sheng J, Tian H, Han J, Fan Z, Qian C (2004) A convenient synthesis of α,α'-bis(substituted benzylidene)cycloalkanones catalyzed by Yb(OTf)3 under solvent-free conditions. Synthesis 18:3060–3064

Weber WM, Hunsaker LA, Abcouwer SF, Deck LM, Vander Jagt DL (2005) Anti-oxidant activities of curcumin and related enones. Bioorg Med Chem 13:3811–3820

Weber WM, Hunsaker LA, Gonzales AM, Heynekamp JJ, Orlando RA, Deck LM, Vander Jagt DL (2006) TPA-induced up-regulation of activator protein-1 can be inhibited or enhanced by analogs of the natural product curcumin. Biochem Pharmacol 72:928–940

Zhou J (2003) One-step synthesis of pyridine and 4H-pyran derivatives from bisarylidenecyclohexanone and malononitrile under microwave irradiation. Syn Commun 33:99–103